

## Supporting Information

### Novel Injectable Gallium-based Self-Setting Glass-Alginate Hydrogel Composite for Cardiovascular Tissue Engineering

Owen M. Clarkin<sup>a</sup>, Bing Wu<sup>a,b,c,\*</sup>, Paul A. Cahill<sup>d</sup>, Dermot F. Brougham<sup>c</sup>, Dipanjan Banerjee<sup>b,e</sup>, Sarah A. Brandy<sup>a</sup>, Eoin K. Fox<sup>a</sup>, Caitríona Lally<sup>f</sup>

- a. DCU Biomaterials Research Group, Centre for Medical Engineering Research, School of Mechanical and Manufacturing Engineering, Dublin City University, Dublin 9, Ireland
- b. DUBBLE Beamline, European Synchrotron Radiation Facility (ESRF), 71 avenue des Martyrs, CS 40220, Grenoble 38043, France
- c. School of Chemistry, University College Dublin, Belfield, Dublin 4, Ireland
- d. Vascular Biology and Therapeutic Laboratory, School of Biotechnology, Faculty of Science and Health, Dublin City University, Dublin 9, Ireland
- e. Department of Chemistry, KU Leuven, Celestijnenlaan 200F box 2404, 3001 Leuven, Belgium
- f. Department of Mechanical and Manufacturing Engineering, School of Engineering, Trinity College Dublin, Dublin 2, Ireland

Corresponding Author Email: [bing.wu@esrf.fr](mailto:bing.wu@esrf.fr)

## **S1. Experimental Setting:**

### **S1.1 Particle Size Analysis**

Particle size analysis was carried out using a 632.8 nm He-Ne laser Malvern Mastersizer 3000 (Malvern, UK). Particles were pre-sonicated (15 seconds) and analysed in a 100% methanol dispersion medium (obscuration: 2.50-3.50 %, measured range: 0.01-3500  $\mu\text{m}$ ).

### **S1.2 Comparison Material**

12w/v % ethylene vinyl alcohol (EVOH) was dissolved in 88% dimethyl sulfoxide (DMSO) by heating to 60°C and stirring until fully dissolved. This solution was then allowed to cool and poured into molds of appropriate dimensions before being placed into an aqueous solvent (DMEM) to allow the material to set.

### **S1.3 Fourier Transform Infrared Spectroscopy**

Gels were produced as described previously. Heavy water ( $\text{D}_2\text{O}$ ) was substituted for  $\text{H}_2\text{O}$  to avoid overlapping of the infrared absorption band of free water with the carboxyl group of the gel. Samples were flash frozen in liquid nitrogen (-196 °C) 10 seconds, 60 seconds, 5 minutes, 60 minutes and 24 hours after mixing. Frozen samples were placed immediately in a lyophilization chamber under vacuum to dry. The 24 hour sample was placed in a small parafilm-sealed Eppendorf centrifuge tube and incubated at 37 °C before being lyophilized. Lyophilized gels were ground and 100 mg was mixed with 400mg potassium bromide (KBr) and placed in a Perkin Elmer Spectrum GX with a blank KBr background sample. Spectrums were collected between 4000 and 400  $\text{cm}^{-1}$  with an accumulation number of 32, a resolution of 4  $\text{cm}^{-1}$  and interval of 1.0  $\text{cm}^{-1}$ . Originlab (Northampton, Massachusetts, USA) was used to perform a baseline subtraction *via* a modified Savitzky-Golay algorithm and a cubic B-spline fitting routine.

### **S1.4 Injectability Testing**

Hydrogel samples were prepared as described previously and were immediately placed in a borosilicate glass syringe (Fisher Scientific, Ireland) fitted with a 21 gauge needle and held in place using a specially designed aluminium stand (Figure S8 inset). The syringe was depressed using a 5kN Zwick BT1-FR005TN test machine fitted with a 500 N load cell. Samples were loaded at 5 mm/min 7, 9, 11, 13 and 15 minutes after mixing and data was recorded using TestXpert software (v.11.02) (Zwick, Ulm, Germany). Load-displacement graphs were plotted and maximum acceptable force was considered to be 25N.

### **S1.5 X-ray Diffraction**

Powdered glass samples were analysed using Cu K $\alpha$ 1 radiation (40kV, 35Ma) in a Brüker D8 Advance X-ray diffractometer (Brüker, Billerica, Massachusetts, USA). Diffractograms were collected in the range of  $10^\circ < 2\theta < 80^\circ$ , at a scan step size of  $0.1^\circ$  and a step time of 5.0 s.

### **S1.6 Differential Thermal Analysis**

A Stanton Redcroft STA 1640 differential thermal analyser (Rheometric Scientific, Epsom, England) was used to measure the glass transition temperature ( $T_g$ ) of each glass. Glasses were heated in air ( $900^\circ\text{C}$  at  $10^\circ\text{C min}^{-1}$ ) using a blank matched platinum crucible used as a reference.

### **S1.7 Solid State Nuclear Magnetic Resonance Analyses**

Powder samples of glasses were analysed using a 14.1 T Bruker Advance III NMR spectrometer (Bruker, Billerica, Massachusetts, USA) equipped with a 4mm CP-MAS probe.  $^{29}\text{Si}$ ,  $^{27}\text{Al}$ ,  $^{71}\text{Ga}$  and  $^{31}\text{P}$  NMR spectra were recorded at resonance frequencies of 119.2 MHz, 156.3 MHz, 183 MHz and 243MHz, respectively. The rotor was spinning at 10 kHz. The  $90^\circ$  pulse lengths were 4.0, 3.5, 2.7 and 3.8  $\mu\text{s}$ , for  $^{29}\text{Si}$ ,  $^{27}\text{Al}$ ,  $^{71}\text{Ga}$  and  $^{31}\text{P}$ , respectively. The recycle times were 1.0 min in each case. The reference materials used to calibrate chemical shifts were  $\text{Si}(\text{CH}_3)_4$ ,  $\text{Al}(\text{NO}_3)_3$ ,  $\text{Ga}(\text{NO}_3)_3$  and  $\text{H}_3\text{PO}_4$  (85% aqueous solution).

### **S1.8 Extended X-ray Absorption Fine Structure (EXAFS) Analyses**

The X-ray absorption near-edge structure (XANES) analyses and the Extended X-ray Absorption Fine Structure (EXAFS) spectra of Ga K-edge (10367 eV) were collected for each sample at the Dutch-Belgian Beamline (DUBBLE, BM26A) (Nikitenko et al., 2008) at the European Synchrotron Radiation Facility (ESRF). The energy of the X-ray beam was tuned by a double-crystal monochromator operating in fixed-exit mode using a Si(111) crystal pair. Measurements were performed in transmission mode with N<sub>2</sub>/He and Ar/He filled ionization chambers. Two scans were collected for each sample to check for reproducibility and these were averaged to increase the signal/noise ratio of the spectra. Energy calibration was performed by measuring the EXAFS spectrum of Ga metal foil. The EXAFS spectra, several scans per sample, were energy-calibrated and were further analyzed using WinXAS (Ressler, 1997). Standard procedures were used for pre-edge subtraction and data normalization in order to isolate the EXAFS function ( $\chi$ ). The isolated EXAFS oscillations, accomplished by a smoothing spline as realized in the program WinXAS (Ressler, 1998), were k<sup>3</sup> – weighted and Fourier transformed over the k-range from 2 to 13 Å<sup>-1</sup> using a Bessel window function. The data were fitted using the ab initio code FEFF 8.2 (Newville, 2001) which was used to calculate the theoretical phase and amplitude functions that subsequently were used in the non-linear least-squares refinement of the experimental data. Only the first peak of the Fourier transformed spectra was fitted in order to determine the Ga-O coordination environment.

### **S1.9 Pycnometry**

Density of each glass was determined using a Micromeritics helium pycnometer (Micromeritics Instrument Corp., Norcross, Georgia, USA). 25 runs were used to determine the average density of each glass (3.0-5.0 g of glass, 12 cm<sup>3</sup> chamber), using a blank chamber as a reference.

### **S1.10 Inductively Coupled Plasma – Atomic Emission Spectroscopy**

Elution samples were carried out as previously described. 100 µl of eluent was removed from five separate samples and each was diluted to 50 ml in 2% HNO<sub>3</sub>. Each sample was run with a minimum of three calibration concentrations for each elemental standard. ICP-AES was carried out on a Liberty 220 Emission Spectrometer (Agilent, Santa Clara, USA) at a coil power of 1.1kW using argon gas as a carrier.

### **S1.11 Platelet Adhesion Analysis**

Fresh bovine blood was acquired at slaughter in a 3 parts trisodium citrate solution (3.8 wt.%) to 20 parts blood. Blood was centrifuged at 200g for 20 minutes at 22°C and a platelet rich plasma (PRP) was collected from the supernatant. Half the PRP was centrifuged at a g force of 1000 for 15 min to obtain the platelet poor plasma (PPP) from the supernatant. A platelet count was carried out from the PRP using a hemocytometer and diluted to  $0.35 \times 10^8$  platelets/ml with PPP. 0.271 mg of Quinacrine mustard dihydrochloride (mepacrine) (10 µmol/L) was added to 50 ml of the platelet suspension and allowed to sit in the dark for 30 minutes at 37°C. Samples (hydrogels and Ti<sub>6</sub>Al<sub>4</sub>V controls) were placed at the base of 6 well plates and 2 ml of platelet solutions were added to each well, ensuring that samples were fully immersed. Samples were incubated in the platelet containing solutions under static condition for 60 minutes at 37 °C, 5 % CO<sub>2</sub> and rinsed twice with PBS in order to remove the platelets which were not attached to the material surface. Adhered platelets were fixed by immersing samples in 2% and 5% glutaraldehyde solutions for 2 h each. Environmental scanning electron microscopy was carried out using a Carl Zeiss (Jena, Germany) EVO LS 15 scanning electron microscope, at a high relative humidity by incorporating a Deben (Suffolk, UK) cold sample stage. Secondary electron images were obtained of the surface of gels and controls. Fluorescence microscopy was carried out on an Olympus BX51 (Tokyo, Japan) at an excitation wavelength of 488 nm and captured using CellF software (Olympus).

### **S1.12 Statistical Analysis**

One way analysis of variance (ANOVA) was performed to determine significant affects across groups and comparison of means was performed using the post-hoc Bonferroni correction t-test. Differences between groups was deemed significant when  $p \leq 0.05$ . All statistical analysis was carried out using SPSS Statistics 23 (IBM, Armonk, New York).

## **S2. Additional Results and Discussions:**

### **S2.1 NMR and EXAFS Characterization of the glasses**

To evaluate the chemical environment of the glasses, solid-state NMR spectra were recorded for the different nuclei present. The  $^{27}\text{Al}$  MAS-NMR spectra of the AL100 glass (**Fig. S2A**), exhibits three different aluminium coordination sites; tetrahedral coordination, Al(IV), at c.60 ppm, pentahedral coordination Al(V) at c.38 ppm, and octahedral coordination, Al(VI) at c.6 ppm as reported in previous studies, (Bunker, Kirkpatrick, & Brow, 1991; Iftekhhar, Grins, Gunawidjaja, & Eden, 2011; Stebbins, Kroeker, Lee, & Kiczinski, 2000). As shown in **Table S1** and **Figure S1**, the Al site distribution changes on substituting with Ga, suggesting a different site preference for the latter ion. It is found that with increasing gallium content, the ratio between Al(IV) and  $[\text{Al(V)} + \text{Al(VI)}]$  is reduced. On the other hand, the average Ga-O in all the cases are approximately 1.83 Å, which suggests a tetrahedral Ga-O coordination, as suggested in a previous study on  $\beta\text{-Ga}_2\text{O}_3$  (Geller, 1960). Ga K-edge EXAFS spectra (**Fig. S2C** and **S2D**) and the fitting results from the first peak in the Fourier transformed spectra (**Table S2**) reveal that there are different Ga-O distances in the first coordination shell of Ga, one Ga-O distance is shorter ( $\sim 1.80$  Å) whereas three other Ga-O distances are longer ( $\sim 1.85$  Å) suggesting a distorted tetrahedral coordination environment for Ga as reported before in similar materials (Hee et al., 2014).

As can be observed from Figure 3B, the  $^{29}\text{Si}$  MAS-NMR spectra are similar for all glass compositions. The broad  $^{29}\text{Si}$  resonance is centred around -80 ppm, which is in the expected

range for Q<sup>2</sup>/Q<sup>3</sup> structured silicon. The slight positive shift with increasing Ga content indicates the preference of Ga tetrahedral coordination as demonstrated in EXAFS analyses.

## S2.2 Disadvantages of Using Other Gelating Agents

Calcium chloride (CaCl<sub>2</sub>) leads to poorly controlled gelation due to its high solubility, resulting in inhomogeneous gels with poor mechanical properties (Shevach, Soffer-Tsur, Fleischer, Shapira, & Dvir, 2014). Less soluble crystalline species, such as calcium sulfate or calcium carbonate, can be used to control the gelation reaction, but the reaction rate cannot be easily modified by varying the crystalline composition or particle size. Furthermore, CaSO<sub>4</sub> results in rapid gelation kinetics that are difficult to control and resulting structures are not uniform (Kuo & Ma, 2001). CaCO<sub>3</sub> is poorly soluble but reduction of pH releases Ca<sup>2+</sup> and generates CO<sub>2</sub> bubbles which make the resulting gels fragile (EP20100711941, 2015). Finally, ion chelators such as sodium hexametaphosphate slow the reaction but have an adverse effect on the mechanical properties and adhesiveness of the gels (Larsen, Bjornstad, Pettersen, Tonnesen, & Melvik, 2015). Hence ion releasing glasses are alternative gelation agents that can provide a route to finely controlled alginate hydrogel gelation rates, through their chemical composition and particle size. We show here that significant quantities of multivalent ions can be released over a prolonged period of time, resulting in a highly crosslinked, homogenous and mechanically stable hydrogel.

**Table S1** Fit parameters for <sup>27</sup>Al NMR Spectra of all the samples

Sample	Al (IV)		Al (V)		Al (VI)	
	Δ (ppm)	Ratio (%)	Δ (ppm)	Ratio (%)	Δ (ppm)	Ratio (%)
AL100	61.6	56.1	36.6	23.4	5.9	20.5
AL067	60.7	58.1	37.0	34.5	8.0	7.4
GA067	57.8	40.3	41.6	49.7	5.7	10.0

**Table S2** Fit parameters for Ga samples (first peak in FT)

Sample	Path	CN	R (Å)	Debye-Waller (σ <sup>2</sup> )
Ga100	Ga - O	1.0	1.82	0.001

	Ga - O	3.7	1.84	0.008
Ga067	Ga - O	0.9	1.76	0.003
	Ga - O	3.6	1.85	0.004
Al067	Ga - O	1.3	1.82	0.008
	Ga - O	3.2	1.84	0.004

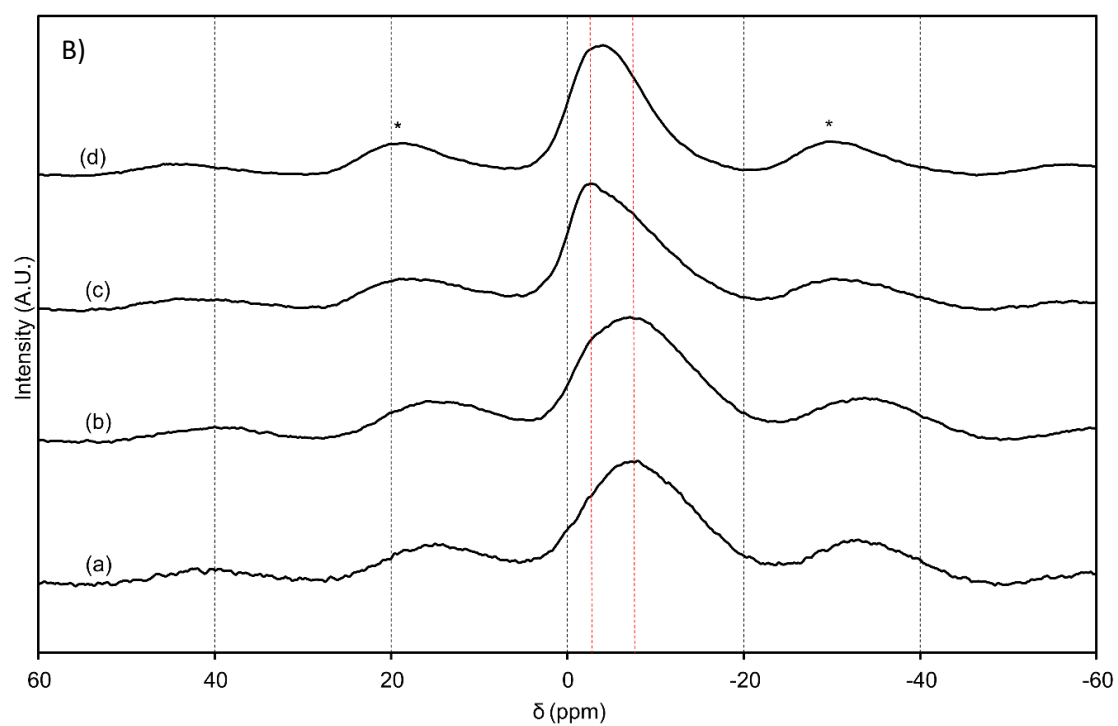
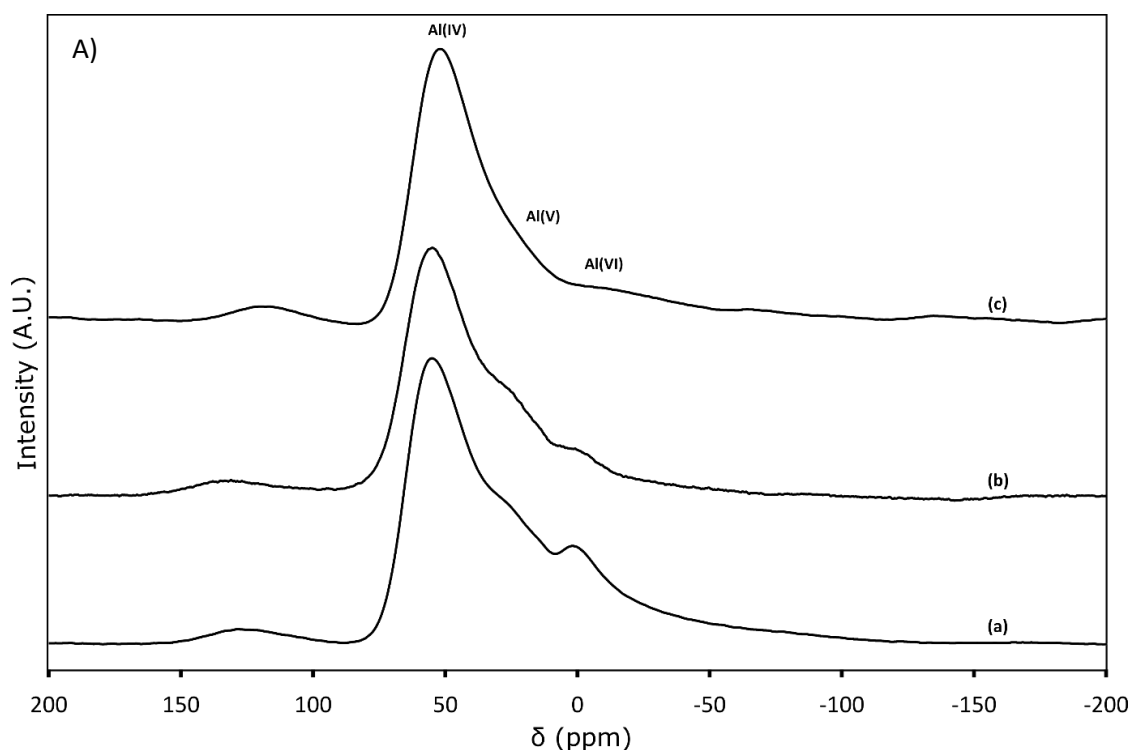




**Figure S1:** **A)**  $^{27}\text{Al}$ -MAS-NMR spectra of samples (a) AL100, (b) AL067, (c) GA067; **B)**  $^{31}\text{P}$ -MAS-NMR spectra of samples (a) AL100, (b) AL067, (c) GA067, (d) GA100.

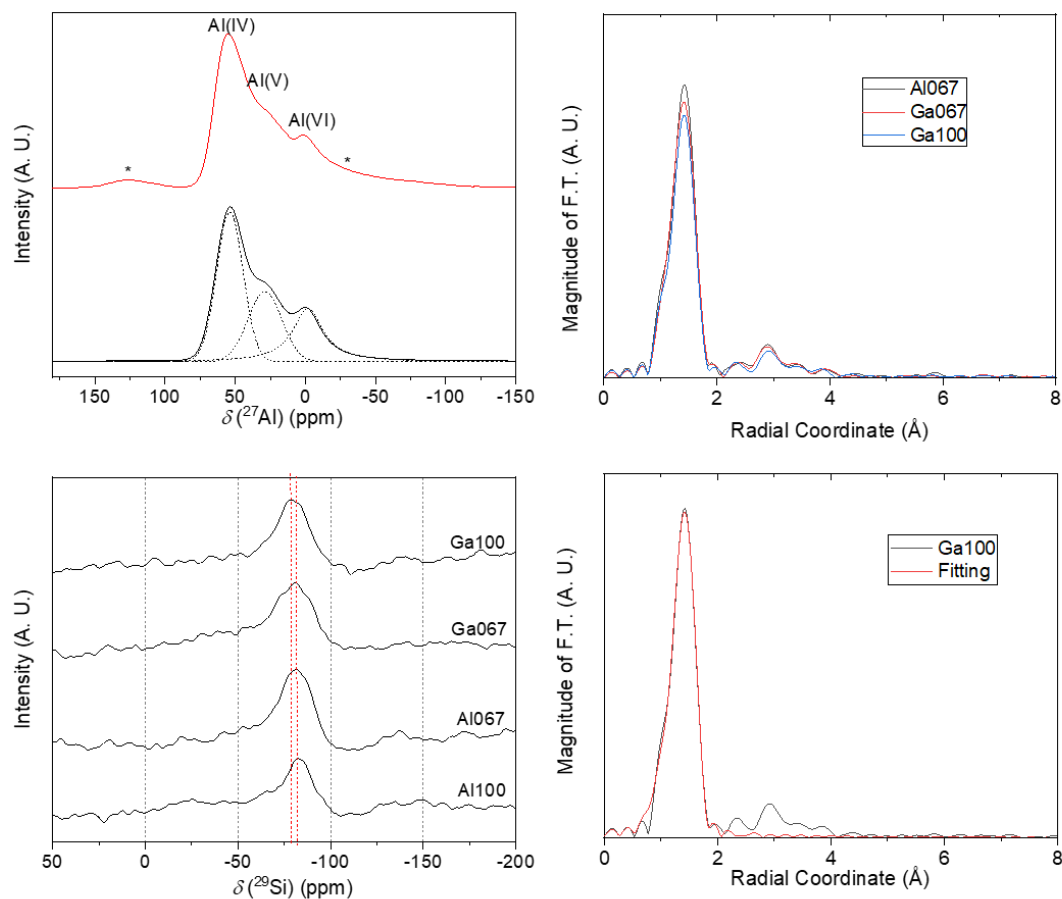


**Figure S2:** Solid State NMR spectra of the glasses; a)  $^{27}\text{Al}$  NMR of AL100 and its fitting; b)  $^{29}\text{Si}$  NMR of all the samples; c) FT Ga K-edge EXAFS Spectra of all the samples; (d) Fitting of FT Ga K-edge EXAFS Spectrum of GA100.

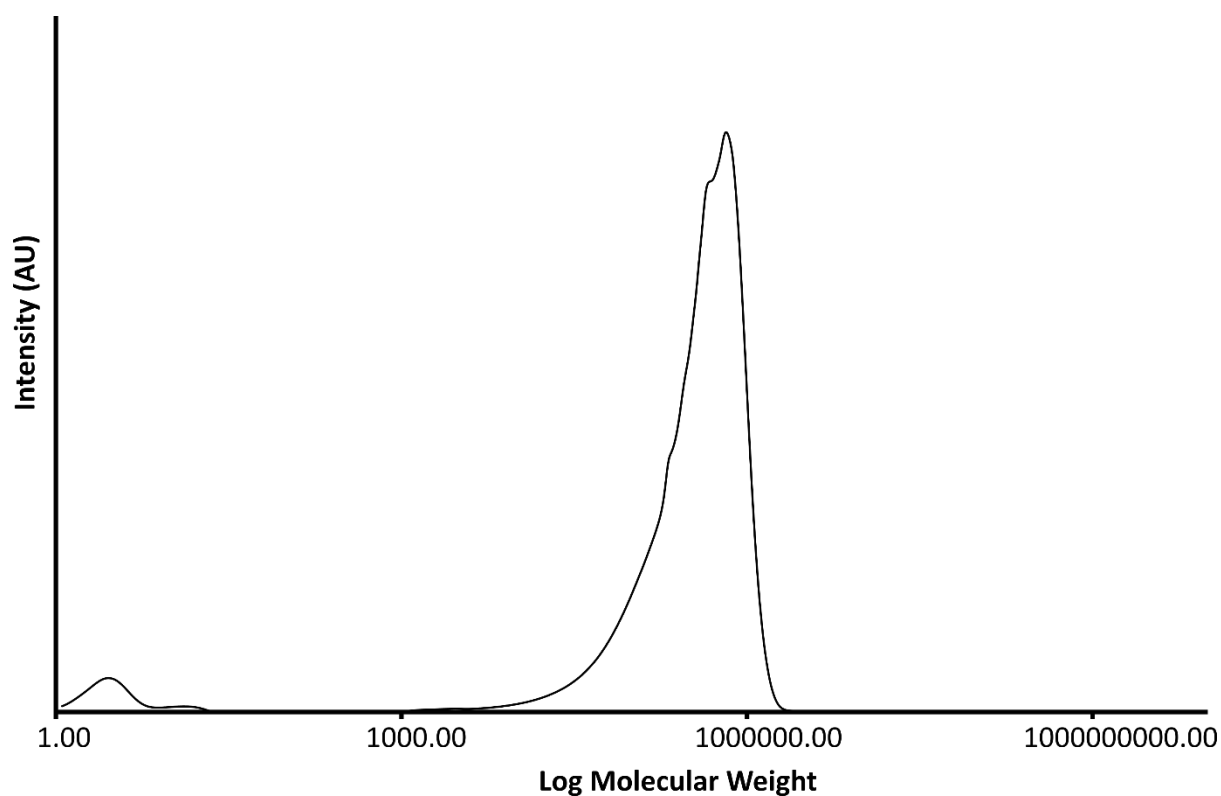


**Figure S3:** GPC spectrum of potassium alginate used in this study.

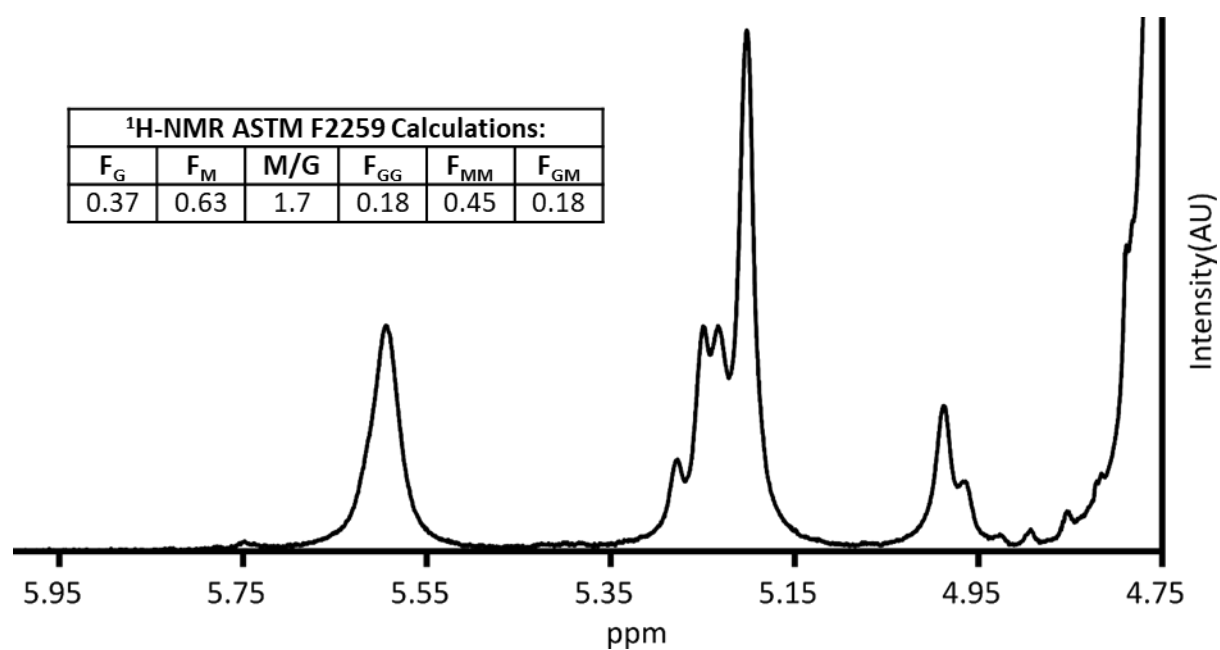


**Figure S4:** <sup>1</sup>H-NMR spectrum of potassium alginate used in this study.

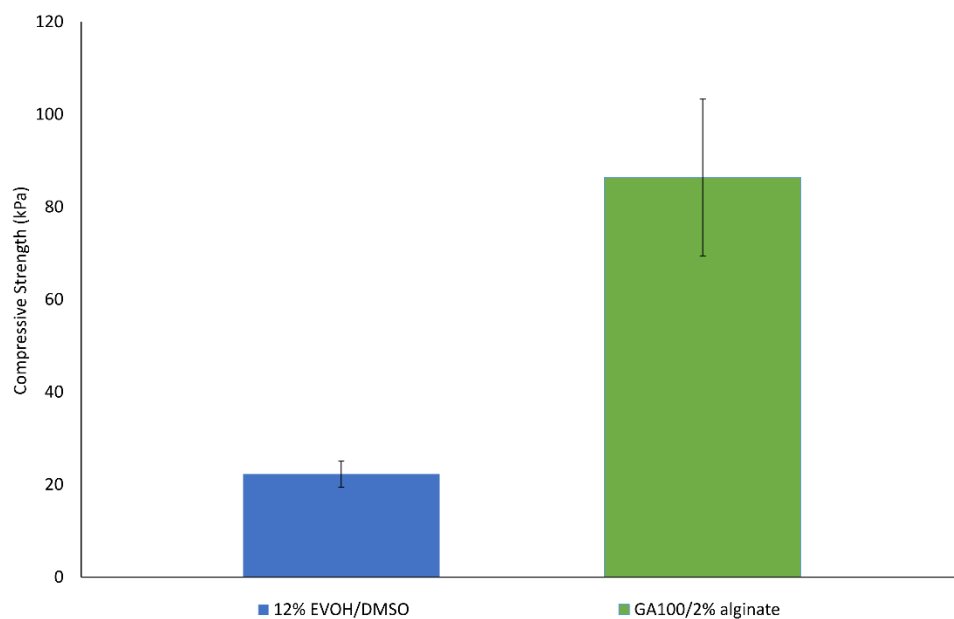


**Figure S5:** Maximum compression stress up to 50% strain, comparison of the GA100 hydrogel after 1 day of immersion in DMEM and a 12wt.% EVOH/DMSO composition.

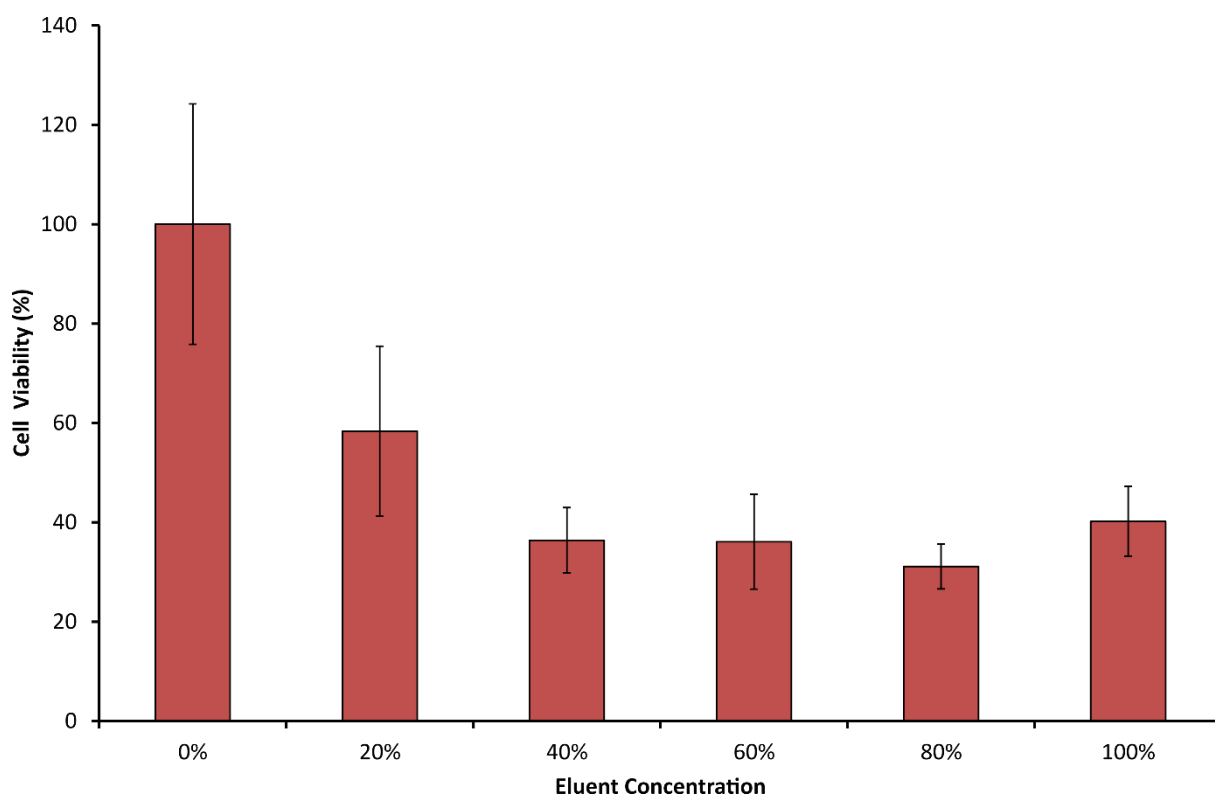


**Figure S6:** BAEC viability after 48 hours when placed in contact with various concentrations of eluent from 12wt% EVOH/DMSO formulation.

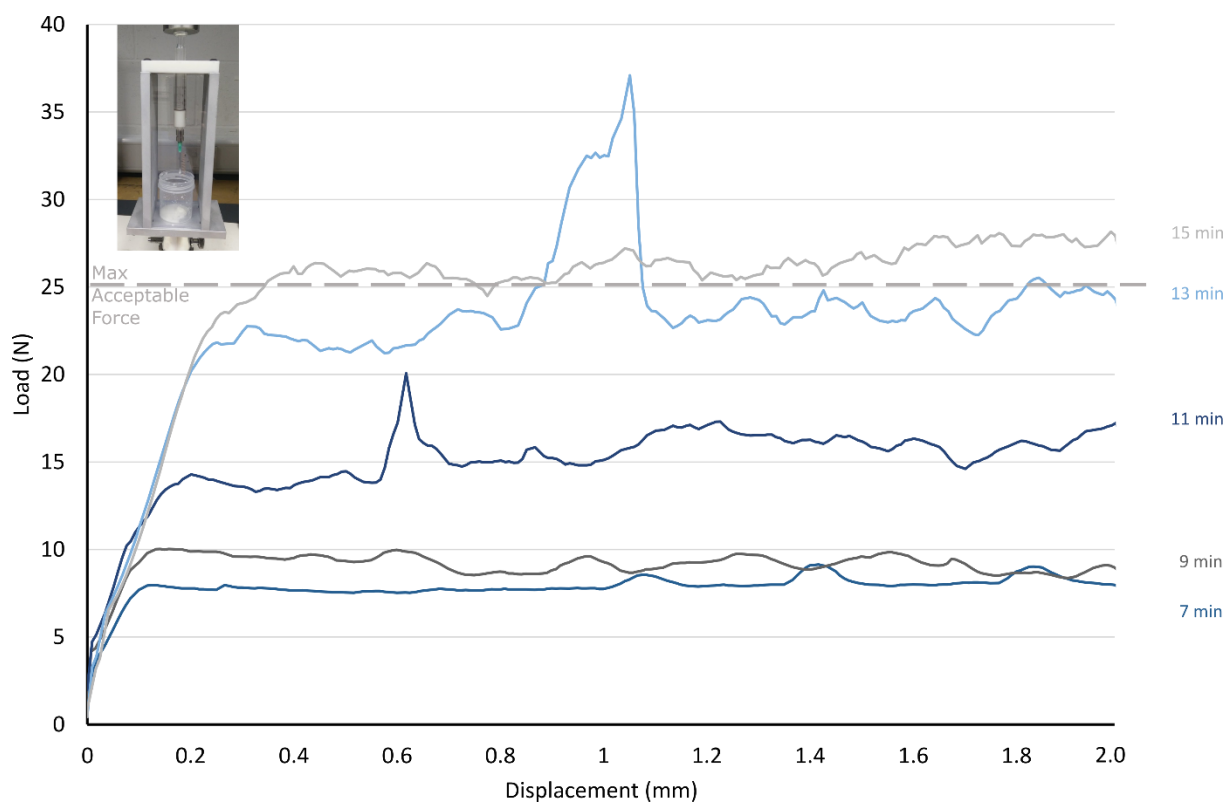


**Figure S7:** Injectability testing through a 21 gauge needle at 5 mm/min at various times.

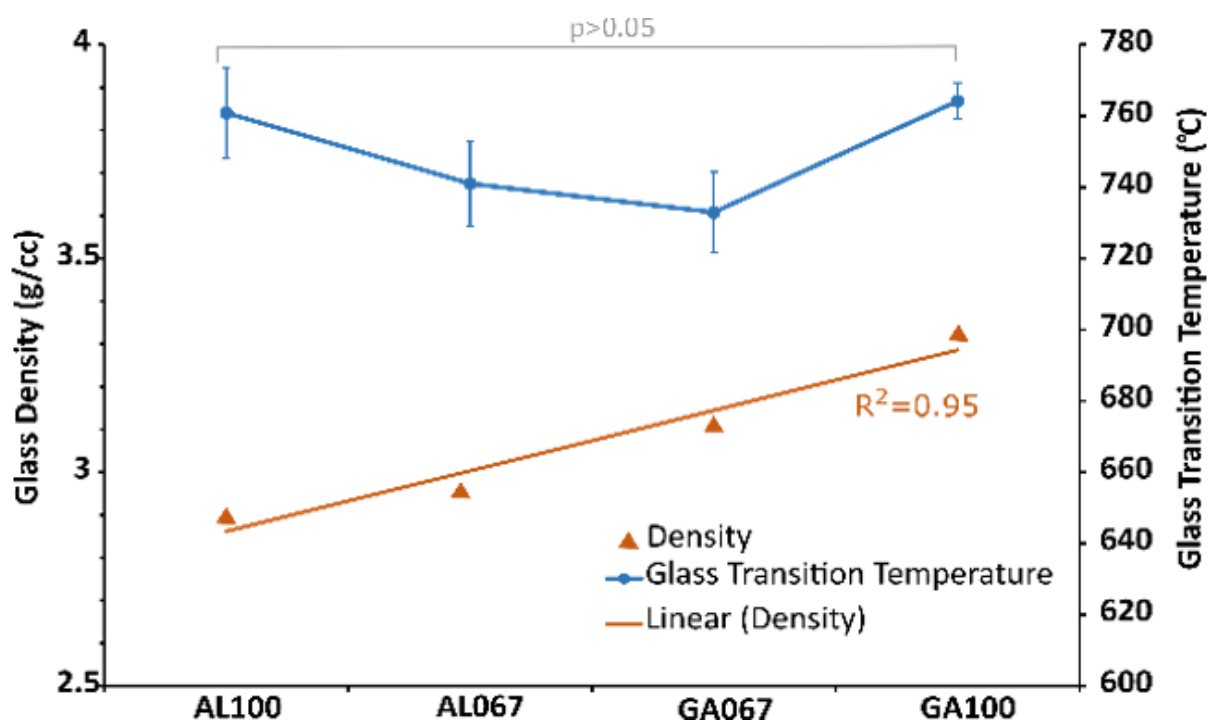


**Figure S8:** density and glass transition temperature of the glass components.

## Ga sample EXAFS Fits

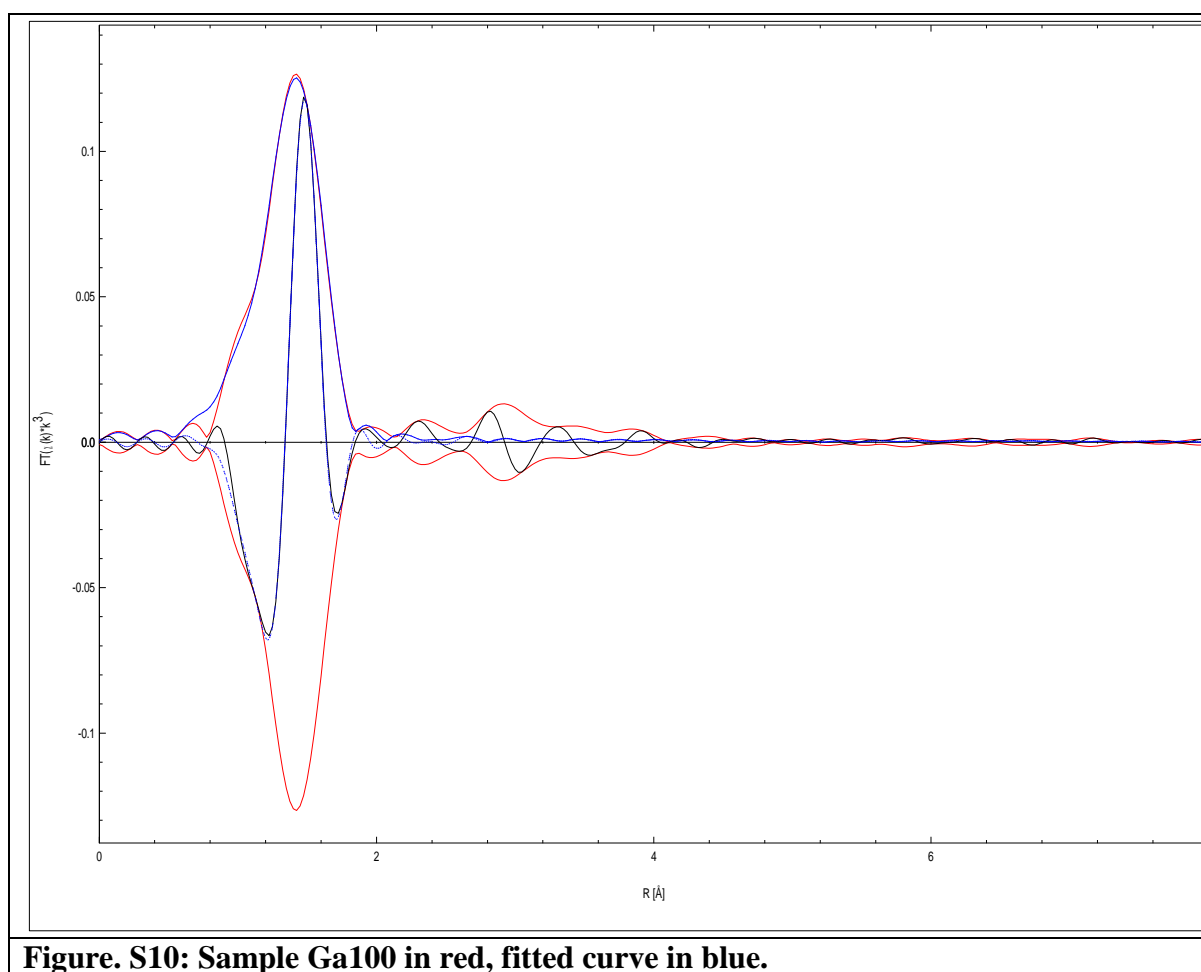


**Figure. S10: Sample Ga100 in red, fitted curve in blue.**

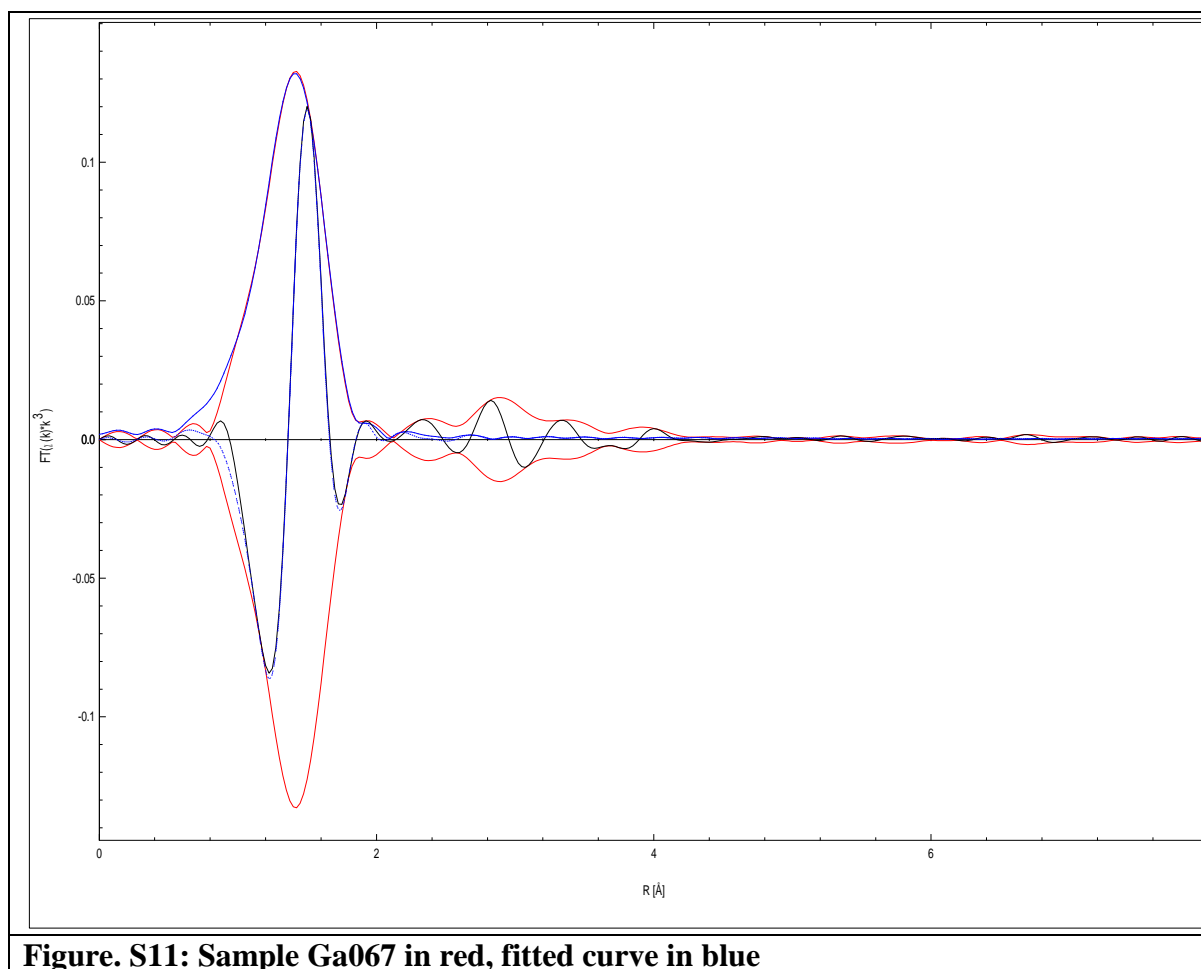


**Figure. S11: Sample Ga067 in red, fitted curve in blue**

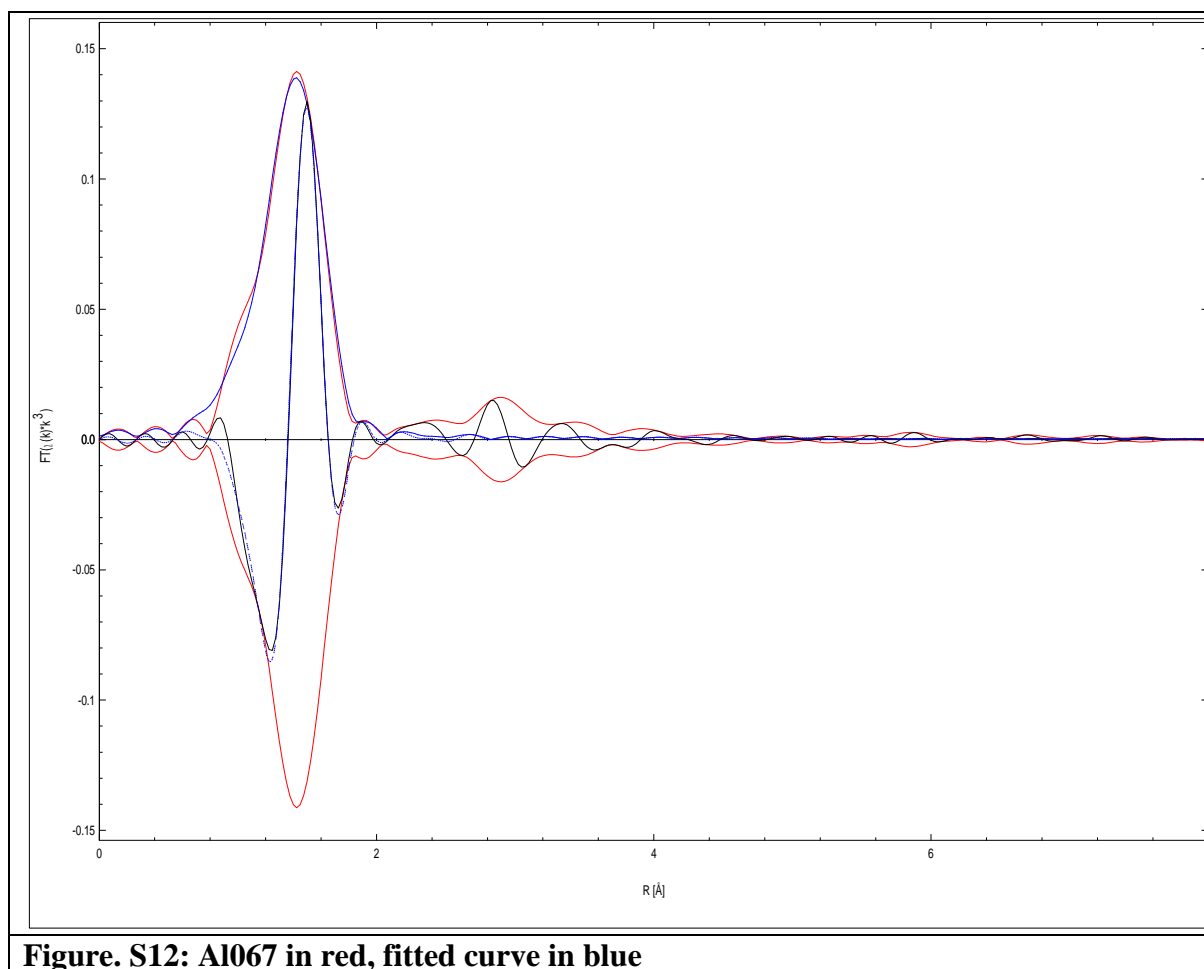


**Figure. S12: Al067 in red, fitted curve in blue**

## References:

- Bunker, B. C., Kirkpatrick, R. J., & Brow, R. K. (1991). Local-Structure of Alkaline-Earth Boroaluminate Crystals and Glasses .1., Crystal Chemical Concepts Structural Predictions and Comparisons to Known Crystal-Structures. *Journal of the American Ceramic Society*, 74(6), 1425-1429.
- Geller, S. (1960). Crystal Structure of Beta-Ga<sub>2</sub>O<sub>3</sub>. *Journal of Chemical Physics*, 33(3), 676-684.
- Iftekhar, S., Grins, J., Gunawidjaja, P. N., & Eden, M. (2011). Glass Formation and Structure-Property-Composition Relations of the RE<sub>2</sub>O<sub>3</sub>-Al<sub>2</sub>O<sub>3</sub>-SiO<sub>2</sub> (RE = La, Y, Lu, Sc) Systems. *Journal of the American Ceramic Society*, 94(8), 2429-2435.
- Kuo, C. K., & Ma, P. X. (2001). Ionically crosslinked alginate hydrogels as scaffolds for tissue engineering: Part 1. Structure, gelation rate and mechanical properties. *Biomaterials*, 22(6), 511-521.
- Larsen, B. E., Bjornstad, J., Pettersen, E. O., Tonnesen, H. H., & Melvik, J. E. (2015). Rheological characterization of an injectable alginate gel system. *Bmc Biotechnology*, 15.
- Newville, M. (2001). EXAFS analysis using FEFF and FEFFIT. *Journal of Synchrotron Radiation*, 8, 96-100.
- Nikitenko, S., Beale, A. M., van der Eerden, A. M. J., Jacques, S. D. M., Leynaud, O., O'Brien, M. G., . . . Bras, W. (2008). Implementation of a combined SAXS/WAXS/QEXAFS set-up for time-resolved in situ experiments. *Journal of Synchrotron Radiation*, 15, 632-640.
- Ressler, T. (1997). WinXAS: A new software package not only for the analysis of energy-dispersive XAS data. *Journal De Physique Iv*, 7(C2), 269-270.
- Ressler, T. (1998). WinXAS: a program for X-ray absorption spectroscopy data analysis under MS-Windows. *Journal of Synchrotron Radiation*, 5, 118-122.
- Shevach, M., Soffer-Tsur, N., Fleischer, S., Shapira, A., & Dvir, T. (2014). Fabrication of omentum-based matrix for engineering vascularized cardiac tissues. *Biofabrication*, 6(2).
- Stebbins, J. F., Kroeker, S., Lee, S. K., & Kiczenski, T. J. (2000). Quantification of five- and six-coordinated aluminum ions in aluminosilicate and fluoride-containing glasses by high-field, high-resolution Al-27 NMR. *Journal of Non-Crystalline Solids*, 275(1-2), 1-6.